Nanotechnol. Environ. Eng. (2017) 2:15
https://doi.org/10.1007/s41204-017-0025-8

ORIGINAL PAPER

A comprehensive review on synthesis and characterizations of Cu_3BiS_3 thin films for solar photovoltaics

Sampat G. Deshmukh[1] · **Vipul Kheraj**[1]

Received: 28 February 2017 / Accepted: 21 July 2017 / Published online: 7 August 2017

Abstract Since the last few decades, light-absorbing materials based on $CuInGaSe_2$ (CIGS), $CuInS_2$ (CIS), and CdTe have dominated the research in thin-film solar cells. To fabricate large-scale solar cells from these materials, problems may arise due to limited availability of the constituents, viz. Se, In, Cd, and Te, and the toxicity of some of these elements. Hence, recent research efforts are attentive toward abundantly available non-toxic, larger value of absorption coefficient and non-conventional elements. The Cu_3BiS_3 having wittichenite orthorhombic structure is one the most promising absorber layer candidates for low-cost thin-film solar cells. It has suitable direct band gap (1.10–1.86 eV), large absorption coefficient (10^5 cm^{-1}) with composition of earth abundant, and relatively non-toxic and cost-effective constituents. Till now, a majority work was done on the preparation of Cu_3BiS_3 thin films by various techniques. Therefore, a comprehensive review of recent literature of Cu_3BiS_3 is urgently required. This paper will review the various techniques that have been used to deposit Cu_3BiS_3 semiconductor with the hope of new paths for the beginner.

Keywords Cu_3BiS_3 · Vacuum and non-vacuum techniques · SEM · Solar cell

✉ Vipul Kheraj
vipulkheraj@gmail.com

Sampat G. Deshmukh
deshmukhpradyumn@gmail.com

[1] Department of Applied Physics, Sardar Vallabhbhai National Institute of Technology, Ichchhanath, Surat, Gujarat 395007, India

Introduction

The thin-film-based solar cell (TFSC) generally use polycrystalline copper indium diselenide (CIS), cadmium telluride (CdTe), or copper indium gallium selenide (CIGS) for commercialization with reported conversion efficiency ranging from 14.6 to 22.3% [1–4]. However, there are limitations to use these materials in the production of photovoltaic (PV) devices as an absorber layer due to toxicity of Cd and Se as well as limited availability of Te, Cd and In [5]. Bismuth is non-toxic and easily available as compared to indium. The US Geological survey assessed in 2014 reported that the world mine production of Bi is 7600 metric tons with world reserves of 320,000 metric tons as compared to In refinery production of 770 metric tons with no estimate of reserves. The cost of Bi in 2013 was $17.4 per kg, while for In it was $620 per kg [6]. Therefore, current research attentions are directed towards an absorbent material that is non-toxic, convenient, and cost-effective. In this context, Cu_3BiS_3 ternary semiconductor compound has emerged as one of the promising candidates for solar absorber material. All the constituents of Cu_3BiS_3 are low cost, non-toxic, earth abundant, and environmentally friendly.

Basics of Cu_3BiS_3 compound and solar cells

The compound Cu_3BiS_3 has been found in nature as the mineral wittichenite, from the Wittichen mine [7]. In the mineral form, the structure (Fig. 1) of the Cu_3BiS_3 compound has been determined as orthorhombic ($P2_12_12_1$: space group no.19) with $a = 7.723$ Å, $b = 10.395$ Å, and $c = 6.716$ Å [8]. The density of the synthesized Cu_3BiS_3 is 6.01×10^3 kg/m^3 and calculated mass density is

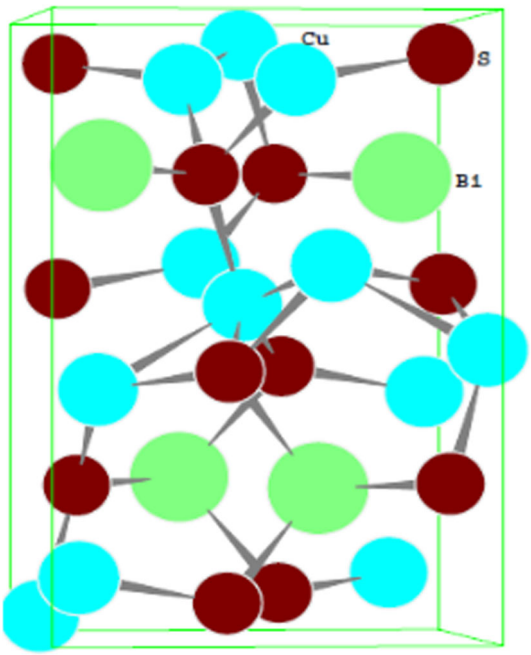

Fig. 1 The crystal structure of Cu_3BiS_3 compound (Taken from [8])

6.11×10^3 kg/m^3, the same as that of an ideal cell dimension with 4 (Cu_3BiS_3) per cell [9]. Cu_3BiS_3 is a ternary compound of I_3–V–VI_3 and is a key member of the copper-based multicomponent chalcogenides (CBMC) family. Cu–Bi–S system alloys are made up of 13 compounds due to variation in the stoichiometric ratio of three elements, which are stable at room temperature [10]. More importantly, Cu_3BiS_3 has a *p*-type conductivity, stronger absorption coefficient (>10^5 cm) [11] in the visible wavelength region and a direct band gap of 1.10–1.86 eV [12, 13]. The copper–bismuth–sulfide forms in several different phases. The phase diagram of the Cu–Bi–S system at 573 K is shown in Fig. 2 [14]. The investigation on the phase diagram of the Cu–Bi–S system has shown that a single-phase Cu_3BiS_3 material can be formed only in a small region.

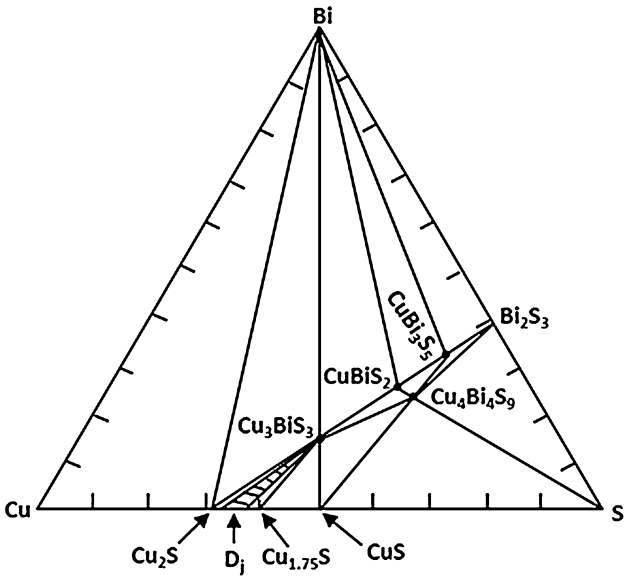

Fig. 2 Phase diagram of Cu–Bi–S system at 573 K [14]

For the synthesis of Cu_3BiS_3 thin films as a light absorber, many physical and chemical techniques have been employed, such as sputtering, thermal evaporation, spray pyrolysis technique, electrodeposition, solvothermal, cyclic microwave radiation, hydrothermal, facile biomolecule-assisted solvothermal, hot injection solution, and chemical bath deposition (CBD) technique respectively. The purpose of employing these methods is to develop a low-cost and highly efficient absorber layer for Cu_3BiS_3 thin-film solar cell. In the recent years, many research groups have studied the synthesis and characterization of Cu_3BiS_3 and few of them showed applications in thin-film solar cells. Therefore, all the different techniques employed for the synthesis of Cu_3BiS_3 thin films are summarized in this review.

The device configuration of SLG/Mo/Cu_3BiS_3/CdS/ZnS/Al:ZnO thin-film-based solar cell to study the PV performance is as shown in Fig. 3. The device consists of Mo-coated soda lime glass (SLG), an electrical contact, a layer of Cu_3BiS_3 as a light absorber layer which is in contact with *n*-type CdS or ZnO to form a *p*–*n* junction and thin-layer Al:ZnO on the top of the buffer layer playing the role of a window layer and electrical contact.

Synthesis techniques of Cu_3BiS_3

The techniques for the synthesis of Cu_3BiS_3 thin films can be classified into two categories: vacuum- and non-vacuum-based techniques. According to the method used for the synthesis of Cu_3BiS_3, each technique has a few sub classifications.

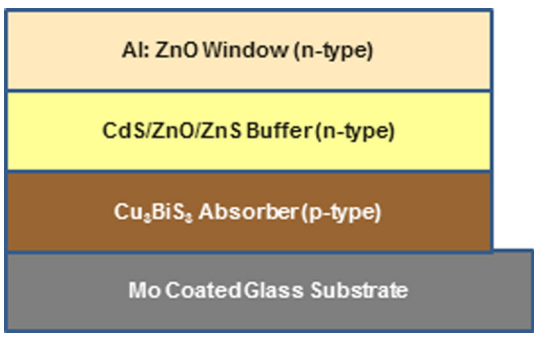

Fig. 3 Schematic structure of Cu_3BiS_3 thin-film-based solar cell

Vacuum-based deposition techniques

Vacuum-based deposition methods normally involve deposition of the constituent atoms of the Cu_3BiS_3 compound on a substrate either by evaporation/co-evaporation or by sputtering of the target sources under optimized pressure and temperature. These techniques have the benefit of fabrication of high-quality thin-film devices, good reproducibility, and easy and direct control over the chemical composition of the sample. These vacuum-based deposition methods can be sub-classified into sputtering, evaporation/co-evaporation, etc.

Vacuum-based sputtering deposition method

To deposit high-quality thin films, many researchers have used sputtering deposition technique. Different sputtering technologies viz. ion beam, argon beam, DC, RF, and reactive magnetron sputtering have been employed for the deposition of Cu_3BiS_3 thin films [11, 15–17]. Cu_3BiS_3 thin films have been deposited using two different methodologies: a single step without sulfurization and a two-step deposition of either metallic precursor Cu–Bi/Cu–S–Bi followed by a sulfurization.

In 2006, Gerein and Haber [15] for the first time deposited Cu_3BiS_3 thin films by sputtering. The Cu_3BiS_3 thin film was synthesised in an H_2S atmosphere where Cu–Bi metal precursor films and Cu–S–Bi metal sulfide precursor films were sputter deposited on fused silica substrate. It was reported that pure orthorhombic phase was obtained at the film thickness of 250–1000 nm. It is also observed that the precursor composition determines the reaction pathway which becomes the dominant factor in controlling the morphology of Cu_3BiS_3 thin films. The deposited Cu_3BiS_3 film had electrical resistivity ranges from 3 to 200 Ω cm. Later on, the same research group [11] reported the synthesis of Cu_3BiS_3 thin films on fused silica substrates in one-step process by reactive sputtering of Cu–S and Bi on hot substrates. The produced thin films of Cu_3BiS_3 are of crystalline phase, smooth, dense, and continuous with direct band gap of 1.4 eV, an absorption coefficient of 1×10^5 cm^{-1}, *p*-type conductivity and electrical resistivity of 84 Ω cm. It is also reported that the crystallite size increased and electrical resistivity decreased to 9.6 Ω cm when Cu_3BiS_3 films are annealed in H_2S atmosphere.

Yakushev et al. [16] fabricated the Cu_3BiS_3 thin films by using magnetron sputtering in two-steps. At first, 0.3 μm thick precursor layers of Cu and Bi were sputtered on Mo-coated SLG from 5 N purity elemental targets. Thick films of 4 N purity sulfur of thickness 1.5 μm were thermally evaporated on these precursor layers followed by heating at 250 °C for 30 min in Ar atmosphere. The synthesized Cu_3BiS_3 thin film had orthorhombic structure, four Raman modes with dominant peak at 292 cm^{-1}, and two bright, broad emission bands at 0.84 and 0.99 eV in XRD, Raman and photoluminescence spectra, respectively. In 2014, the same research group [17] reported the structural, elemental composition, optical, and electronic properties of *p*-type Cu_3BiS_3 thin films by adopting the similar deposition procedure [16]. The deposited Cu_3BiS_3 thin films exhibit single orthorhombic phase with the stoichiometry $Cu_{3.0}Bi_{0.92}S_{3.02}$, photoreflectivity at 10 K expressed two band gaps at 1.24 and 1.53 eV and two broad bands at 0.99 and 0.84 eV in low-temperature PL spectra [17].

Vacuum-based evaporation deposition method

Evaporation techniques are the normal choice of every researcher and being used for the deposition of wittichenite Cu_3BiS_3 absorber due to the previous success of evaporated absorber materials like CdTe [18], CIGS [19], and CZTS [20]. Numerous evaporation methods such as co-evaporation, fast evaporation, thermal evaporation, and electron beam (EB) [21–32] have been employed for the deposition of Cu_3BiS_3 thin films. Cu_3BiS_3 thin films were deposited using two different attitudes:

1. a single-step: simultaneous deposition of all precursors followed by sulfurization
2. a two-step: sequential deposition of metallic Cu–Bi–Cu–S or CuS–Bi_2S_3, Bi_xS_x–Cu followed by a annealing/sulfurization.

First time, in 2009 Mesa and Gordillo [21] reported preparation of Cu_3BiS_3 thin films on a SLG substrate by co-evaporation in a two-step process. In the first step, Bi_xS_x layer was developed by simultaneous evaporation of Bi and S, keeping the substrate temperature at 300 °C. In the second step, Cu_3BiS_3 was formed by evaporating Cu in the sulfur environment on the Bi_xS_x layer at 300 °C. The XRD revealed that the film grown only in the orthorhombic Cu_3BiS_3 phase. The deposited Cu_3BiS_3 thin film had a *p*-type conductivity, a high absorption coefficient ($>10^4$ cm^{-1}), and optical energy gap 1.41 eV, indicating Cu_3BiS_3 had best property to perform as an absorber layer in PV solar cell. Furthermore, Mesa et al. [22] deposited Cu_3BiS_3 thin films by a two-step evaporation process on glass substrates. In the first stage, a Bi thin layer was deposited with a flux of about 1 Å/s, and in second stage Cu is evaporated keeping the flux of about 0.8 Å/s. In both stages, S environment was produced by the evaporation of elemental sulfur at temperature of 383 K and substrate was kept at 573 K. It was reported that the energy required a carrier to jump from one localized state to another increased with the temperature and Cu content in the Cu_3BiS_3. The same group later [23] reported the

preparation of Cu_3BiS_3 on SLG substrate in a two-step process by co-evaporation. In the first stage, a Bi_2S_3 layer was grown by simultaneous evaporation of Bi and S by keeping the substrate temperature 300 °C. In the second stage, Cu was evaporated in a sulfur environment over the Bi_2S_3 layer at temperature ~300 °C to form Cu_3BiS_3.

The proposed reaction mechanism for the formation of Cu_3BiS_3 is as follows:

$$\frac{2}{3}S_2 + 2Bi \overset{300\,^{\circ}C}{\rightarrow} Bi_2S_3 \quad (1)$$

$$2Cu + \frac{1}{2}S_2 \rightarrow Cu_2S \quad (2)$$

$$Bi_2S_3 + 3Cu_2S \overset{300\,^{\circ}C}{\rightarrow} 2Cu_3BiS_3 \quad (3)$$

The result revealed that the Cu_3BiS_3 film had *p*-type conductivity, a high absorption coefficient ($>10^4$ cm^{-1}) and energy band gap of 1.39 eV. It was also reported that grain size and electrical conductivity of Cu_3BiS_3 were influenced by the Cu mass ratio. Then, Mesa et al. [24] synthesized thin films of Cu_3BiS_3 by co-evaporation as described earlier [22, 23]. Hall Effect, Seebeck effect, and surface photovoltage (SPV) measurement showed that Cu_3BiS_3 had a *p*-type semiconductor with Hall mobility, free carrier concentration, and thermoelectric power of 4 cm^2/V s, 2×10^{16} cm^{-3} and 0.73 mV/K, respectively. The work function of Cu_3BiS_3 was reported 4.37 ± 0.04 eV before and 4.57 ± 0.01 eV after deposition of In_2S_3.

Later on, Mesa et al. [25] investigated the formation of ZnS, In_2S_3, and CdS buffer layers on Cu_3BiS_3 for application as an absorber layer in solar cell. The Cu_3BiS_3 and ZnS (thickness 200 nm) thin films were deposited by the co-evaporation techniques reported previously [23, 26]. The buffer layer of In_2S_3 was deposited by co-evaporation of In and S on the substrate heated to ~300 °C having thickness ~150 nm. The CdS thin films of thickness ~80 nm were deposited on Cu_3BiS_3 from a solution containing thiourea and cadmium chloride as sources of S^{2-} and Cd^{2+}, respectively. Kelvin probe force microscopy (KPFM) showed the granular structure of the buffer layers with small grains of 20–100 nm and considerably smaller work function distribution for In_2S_3 compared to that of CdS and ZnS. For In_2S_3 and CdS buffer layers, KPFM indicated negatively charged Cu_3BiS_3 grain boundaries. In 2012 Mesa et al. [27] presented the results from a study held on Al/Cu_3BiS_3/Buffer/ZnO, using a high-resolution transmission electron microscopy (HRTEM) with In_2S_3 and ZnS as a buffer layer. The Cu_3BiS_3 was prepared by two-stage co-evaporation process with film thickness of ~1 μm as reported by Mesa et al. [21, 22]. The ZnS buffer layer was deposited by chemical bath deposition (CBD) method using thiourea and zinc acetate as a precursor solution for S^{2-} and Zn^{2+} source, respectively, with ammonia and sodium citrate as complexing agents. In_2S_3 was deposited by co-evaporating In and S on a substrate heated at a temperature 300 °C. The ZnO thin films were deposited at room temperature on glass/Al/Cu_3BiS_3/Buffer system by chemical reaction between ionized zinc and oxygen: Zn^{+}–1e + O^{-} + 1e^{-} → ZnO. The Cu_3BiS_3 deposited on Al has a nanocrystalline structure with grain size around 10 nm. It was reported that the buffer layer of In_2S_3 grows in a polycrystalline nature, whereas ZnS in an amorphous nature. The ZnO layer grew into a wurtzite-type hexagonal structure, used as an optical window layer.

Furthermore, Dussan et al. [28] prepared Cu_3BiS_3 thin films on SLG substrates by evaporating Cu and Bi species in a sulfur environment through a two-stage process by varying the synthesis temperature between 473–573 K. The thermally stimulated current (TSC) spectrum showed three trapping levels around 1.04 eV. In Cu_3BiS_3 semiconductor, these three trapping levels may be associated with the presence of structural defects and unintentional impurities. Thereafter, Murali et al. [29] in 2014 reported the deposition of Cu_3BiS_3 thin films by co-evaporation of the Cu, Bi elemental precursors on a Mo-glass substrate with in situ sulfurization using a quartz effusion cell. The XRD pattern of Cu_3BiS_3/Mo/SLG stack showed Cu_3BiS_3 film was polycrystalline with preferred (131) orientation. The obtained Cu_3BiS_3 film had a high absorption coefficient ($>10^4$ cm^{-1}), an energy band gap of 1.45 eV, and can be used as an absorber layer for a near-infrared photodetector. Then, Mesa et al. [30] presented the electrical properties of co-evaporated Cu_3BiS_3 by varying precursors mass ratio $m_{Cu}/(m_{Cu} + m_{Bi})$ in between 0.43 to 0.49. Hall effect measurement of Cu_3BiS_3 showed that the concentrations of n charge carriers are in the order of 10^{16} cm^{-3} irrespective of the Cu/Bi mass ratio. Also, the mobility of Cu_3BiS_3 (μ is of the order of 4 cm^2 V^{-1} s^{-1}) varies accordingly to the transport mechanism and depended on temperature. From SPV measurement, a high density of surface defects was observed, which can be passivated by superimposing a buffer layer over the Cu_3BiS_3.

Recently, Mesa et al. [31] in 2015 presented the growth of In_2S_3 onto Cu_3BiS_3 and glass substrates by using CBD and co-evaporation. For this, Cu_3BiS_3 thin films were deposited as reported earlier [23] and In_2S_3 films were deposited on Cu_3BiS_3 by co-evaporation of In and S precursors. For CBD growth at 60 °C of In_2S_3, thin film on Cu_3BiS_3, $InCl_3$ and thioacetamide was used as a source for indium and sulfur. The film thickness of In_2S_3 was observed in between 80–170 nm. The XRD showed In_2S_3 films had a higher crystallinity when grew by co-evaporation than by CBD. Also, thin films of In_2S_3 with thickness less than 170 nm deposited by CBD had amorphous nature. However, when increasing the thickness, the films

exhibit two diffraction peaks along (103) and (107) planes of the β-In_2S_3 tetragonal structure. Films of In_2S_3 grown by CBD had better coverage performance being suitable, to use as a buffer layer with lower thickness compared with those prepared by co-evaporation. Estrella et al. [32] reported the formation of Cu_3BiS_3 by heating a chemically deposited CuS thin film on which Bi was thermally evaporated. The possible film formation reaction was $3CuS + Bi \rightarrow Cu_3BiS_3$. For the formation of CuS, 5 ml of $CuCl_2{\cdot}5H_2O$ (1 M), 9 ml of $Na_2S_2O_3$ (1 M), and 10 ml of 0.5 M dimethylthiourea were used, and the deposition was carried out at 60 °C for 5 h. Then, Bi thin film of 100 nm was deposited by thermal evaporation on CuS thin film. The Cu_3BiS_3 thin film had an optical absorption greater than 10^5 cm^{-1}, *p*-type conductivity of 0.03 Ω^{-1} cm^{-1}, mobility lifetime 10^{-6} cm^2 V^{-1}, and photoconductive. Figure 4 shows a graphical representation of the reported band gap energy in eV in different synthesis methods of Cu_3BiS_3.

Non-vacuum deposition techniques

In the last few decades, the majority of the Cu_3BiS_3 thin-film formation had been reported by various vacuum techniques as discussed above. Nowadays, it proved that an inexpensive deposition, thin-film-based solar cells are offered by the majority of non-vacuum methods. The vacuum-based technique consumes a very high energy, suffers from low material utilization, a small area deposition, expensive, and requires sophisticated instruments, whereas non-vacuum deposition techniques are of low cost and convenient for large area deposition, consume low energy, and do not require sophisticated instruments. Therefore, non-vacuum techniques have been developed to synthesis a ternary Cu_3BiS_3 thin film. This includes spray pyrolysis, solvothermal route, hydrothermal, spin coating, electrochemical deposition, and CBD. The same techniques had been widely used for the synthesis of CdTe [33], CIGS [34], and CZTS [35] semiconductor thin films.

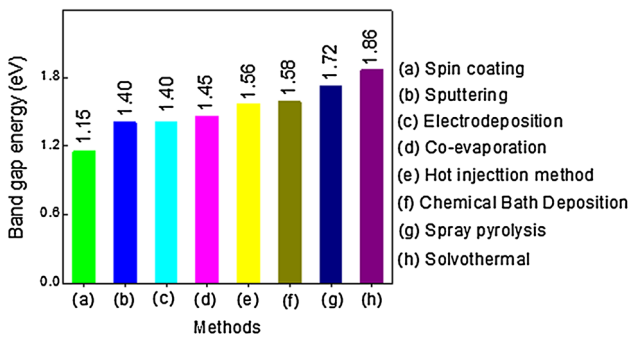

Fig. 4 Band gap energy (eV) of Cu_3BiS_3 reported by various synthesis techniques

The non-vacuum deposition techniques used for the synthesis of Cu_3BiS_3 thin films are listed below:

Spray pyrolysis deposition technique

Spray pyrolysis deposition (SPD) technique does not require vacuum at any stage during the deposition process of thin films of any kind. This method is suitable for mass production with good reproducibility of the films. Considering all these advantages of SPD, attempts have been made in the synthesis of ternary Cu_3BiS_3 thin films. In 2015, for the first time, Liu et al. [36] reported the synthesis of Cu_3BiS_3 thin films by chemical spray pyrolysis technique. A precursor solution which contained 10 mM copper (II) chloride ($CuCl_2$), 3.8 mM bismuth (III) chloride ($BiCl_3$), and 50 mM thiourea in methanol solution was used. The precursor solutions were sprayed onto a heated glass substrate at 250, 300, 350, and 400 °C with solution flow rate 5 ml/min. The XRD pattern showed that as-deposited Cu_3BiS_3 thin films were wittichenite typed. The direct band gap of Cu_3BiS_3 films was reported in the range of 1.65–1.72 eV.

Solvothermal synthesis technique

In solvothermal synthesis technique, the reactions proceed in the thermal (100–300 °C) region so that the reaction velocity is easily controlled. This is favorable for the formation of crystal and to control the crystallite sizes. Therefore, the solvothermal method is suitable for the synthesis of novel nanomaterials with good crystallinity. First time, in 2012 Yan et al. [37] reported a solvothermal route to synthesize good-quality Cu_3BiS_3 nanoparticles at 180 °C for 20 h in a Teflon-lined autoclave containing $Cu(NO_3)_2{\cdot}3H_2O$ (2.42 g), $Bi(NO_3)_3{\cdot}5H_2O$ (0.97 g), and thiourea (1.52 g) dissolved in 25 ml of ethylene glycol (EG). The XRD pattern indicated the phase purity of Cu_3BiS_3 with crystalline grains of ~40 nm. The orthorhombic phase of wittichenite Cu_3BiS_3 with multi-armed microrod morphology was obtained when hypocrellins were used as a template. Then, Zeng et al. [38] successfully synthesized flower-like Cu_3BiS_3 hierarchical nanostructure. In this synthesis, copper chloride dihydrate (0.4276 g), and bismuth chloride (0.1570 g) (stoichiometric ration 3:1) were dissolved into ethanol (35 ml) and glycerol (50 ml) under vital stirring for 20 min, and then thiourea (0.38 g) was added into the solution directly. The whole solution was sealed into a Teflon-lined stainless-steel autoclave and maintained at 180 °C for 12 h. The XRD pattern of Cu_3BiS_3 showed the formation of wittichenite orthorhombic phase. The stoichiometric ratio and band gap of Cu_3BiS_3 thin films was reported 42:12:44 and

1.2 eV, respectively. This synthesized flower-like Cu_3BiS_3 nanostructure may be applied in solar cells.

Further, Murali et al. [39] reported the structural and optical properties of Cu_3BiS_3 nanopowder synthesized by solvothermal. The synthesis of Cu_3BiS_3 nanopowder involved 4 mM copper (II) acetylacetonate, 0.01 M bismuth chloride and 0.1 M thioacetamide into an autoclave at 170 °C for 8 h. It was shown that the obtained Cu_3BiS_3 product had a rod-like structure having the diameter of 60–200 nm and 1–2 μm in length with optical band gap 1.4 eV. Also, the IR photoresponse in-plane geometry was higher compared to sandwich geometry. Later on, Murali and Krupanidhi [13] studied the facile technique to synthesize high-quality Cu_3BiS_3 for photodetector applications. The manufacturing of Cu_3BiS_3 nanopowder by solvothermal at 170 °C for 8 h involved 3 mM CuCl, 0.01 M $BiCl_3$, and 0.1 M $CS(NH_2)_2$ with ethanol as a solvent. The band gap energy of Cu_3BiS_3 particles was varied from 1.86 to 1.42 eV. The Cu_3BiS_3 containing the secondary phases showed relatively higher band gaps. The IR photodetection of Cu_3BiS_3 was also exposed in terms of photocurrent and photoresponse. Furthermore, in 2013, the solvothermal synthesis of Cu_3BiS_3 with precursor complexion was reported by Viezbicke et al. [40]. For the preparation of Cu_3BiS_3, firstly 3 mM $Cu(NO_3)_2{\cdot}3H_2O$ and 3 mM L-cystein was dissolved in 50 mL EG, and then 1 mL $Bi(NO_3)_3{\cdot}5H_2O$ with 1 mM L-cystein was dissolved in separate 50 mL EG with stirring. These two solutions were mixed under stirring into a two-necked flask and heated by mantle at 187 ± 3 °C for 4 h. The XRD pattern confirmed a pure wittichenite [Fig. 5] crystal structure. The synthesized Cu_3BiS_3 had a direct band gap of 1.5 eV. SEM photographs exposed varying morphology dominated by the nanorods and included particles which had aspect ratio 1:1.

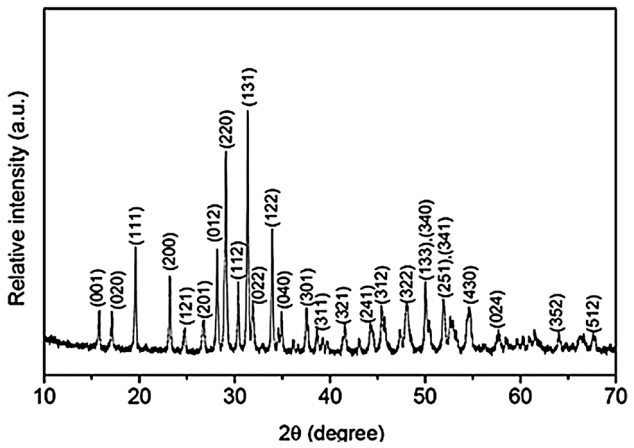

Fig. 5 XRD pattern for pure Cu_3BiS_3 Wittichenite crystal (taken from [40])

Recently, Murali and Krupanidhi [41] reported the preparation and application of Cu_3BiS_3 nanorods in infrared photodetection. The preparation of Cu_3BiS_3 nanorods by solvothermal was described as earlier [13]. They reported that photocurrent was enhanced to threefold from 3.47×10^{-7} to 2.37×10^{-3} A at 1 V for 10 mg nanorods embedded in polymer devices. Responsivity of hybrid device was also enhanced from 0.0158 to 102 A/W. The optical band gap of Cu_3BiS_3 had a value of 1.4 eV. The Cu_3BiS_3 could be promising material in the nano switchable near IR photodetectors. Thereafter, Yin and Jia presented the synthesis and characterization of Cu_3BiS_3 nanosheets on a TiO_2/FTO by solvothermal route. For the preparation of Cu_3BiS_3/TiO_2 composite thin film, CuCl (0.3 mM), $Bi(NO_3)_3{\cdot}5H_2O$ (0.1 mM), and C_2H_6OS (0.6 mM) were added to a mixed solution of glycerol and ethanol (volume ratio 1:1), and synthesis was carried out at 180 °C for 1, 3, and 6 h in an electric oven. Cu_3BiS_3 nanosheets of 30 nm thickness were successfully synthesized on TiO_2 nanorods. The reported energy conversion efficiency of the Cu_3BiS_3/TiO_2 thin-film solar cell was 1.281% [42]. This is the first report on the efficiency of Cu_3BiS_3 thin-film-based solar cell. The flower-like Cu_3BiS_3 was deposited on the TiO_2 nanotubes via a solvothermal method by Zhong et al. [43] at 180 °C for 12 h in an electric oven. The preparative precursor contained $CuSO_4{\cdot}H_2O$, $BiCl_3$ and thiourea at suitable concentrations. Flower-like Cu_3BiS_3 sensitized TiO_2 NTs was successively fabricated. Zhong et al. reported that flower-like structure of Cu_3BiS_3 was composed by nanosheets of thickness 30 nm.

Moreover, Santhanapriya et al. [44] in February 2016 reported the synthesis of Cu_3BiS_3 and Cu_3SbS_3 for different Cu concentrations using EG and triethanolamine (TEA) as a solvent at 180 °C for 20 h. To synthesis Cu_3BiS_3 nanoparticles, $Cu(NO_3)_2$, $Bi(NO_3)_2$, and thiourea were used with EG. The XRD analysis confirmed the pure single-phase orthorhombic structure of Cu_3BiS_3 with an average crystallite size of 38 nm. The FESEM images indicated a flower-like structure and photoluminescence analysis showed strong emission at 455 nm for Cu_3BiS_3.

More recently, Gao et al. [45] reported the solvothermal synthesis of Cu_3BiS_3 for high performance lithium–sulfur batteries. For the synthesis of Cu_3BiS_3, $CuCl_2{\cdot}2H_2O$ (0.4276 g), $BiCl_3$ (0.1570 g) and thiourea (0.38 g) were dissolved in ethanol (35 mL) and glycerol (50 mL), and the reaction was carried out 180 °C for 12 h. The Cu_3BiS_3 had 3D flower-like ball morphology composed by misoriented and 2D thin nanosheets with outer diameter of 1.5–3.0 μm. The XRD of Cu_3BiS_3 3D flower-like ball showed that all the diffraction peaks could be indexed to the orthorhombic phase. It was also shown that the Cu_3BiS_3/S flower exhibited a high initial capacity of 1343 mA h g^{-1} at the

current rate of 0.2C. A high specific capacity of 487 mA h g^{-1} with a coulombic efficiency of 90% could be obtained at 0.2 C after 100 cycles. Figure 6 shows a graphical representation of the maximum reported particle size (nm) in different synthesis methods of Cu_3BiS_3.

Hydrothermal synthesis technique

During the last decade, the chemical solution routes were evolving as an effective, less energy, convenient, and material-consuming synthesis methods for materials synthesis. Hydrothermal method is one of the greatest emergent chemical solution methods owing to its high degree of compositional control of the stoichiometry. Hu et al. [46] reported the synthesis of Cu_3BiS_3 at 100–150 °C for 10 h in an autoclave having precursor solutions CuCl, $BiCl_3$, and thiourea. As-prepared Cu_3BiS_3 consists of whisker-like particles with an average size of 50 × 10 nm^2. The X-ray diffraction profile showed the formation of orthorhombic Cu_3BiS_3 phase with average particle size of about 35 nm. The proposed chemical reaction which describes the formation of Cu_3BiS_3 was given as follows:

$$CuCl + xTu \rightarrow \left[Cu(Tu)_x\right]^{+} + Cl^{-} \quad (4)$$

$$BiCl_3 + yTu \rightarrow \left[Bi(Tu)_y\right]^{3+} + 3\ Cl^{-} \quad (5)$$

$$3\left[Cu(Tu)_x\right]^{+} + \left[Bi(Tu)_y\right]^{3+} \rightarrow Cu_3BiS_3 + (3x + y)Tu \quad (6)$$

Later on, Chen et al. [47] produced the Cu_3BiS_3 nanorods by a simple ethanol-thermal route. For this, appropriate amount of $CuCl_2{\cdot}2H_2O$ (0.005 M), $BiCl_3$ (0.001 M), and thiourea (0.01 M) were added into a Teflon-lined SS autoclave containing ethanol or EG or glycerine up to 80% of total volume, retained at 160 °C for 10 h. Cu_3BiS_3 nanorods with different aspect ratios had been produced using different solvents. It was reported that the ethanol, ethylene glycol, and glycerine solvents were the key factors for the production of Cu_3BiS_3 nanorods. The formation of pure phase of Cu_3BiS_3 with the average crystalline size of nanorods 23 nm was reported from XRD study. TEM analysis showed 35 nm diameter and 2–15 μm length of produced nanorods.

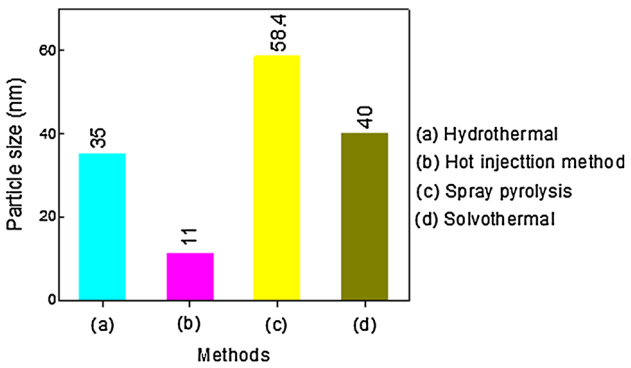

Fig. 6 Maximum particle size (nm) of Cu_3BiS_3 reported by several synthesis techniques

Electrodeposition technique

Electrodeposition is an alternative promising method used for the low-cost synthesis of different semiconductor thin films for a small amount in research as well as large amounts in industry approach. This technique has been widely used for the fabrication of thin-film absorber layer viz. CIGS [48], CZTS [49], and CdTe [50] solar cells. Cu_3BiS_3 films made by an electrodeposition method were firstly reported by Peter et al. [51]. The Cu_3BiS_3 layer was deposited (1–2 μm thick) on the Mo-coated glass from a solution containing $Bi(NO_3)$ (9 mM), $CuSO_4{\cdot}H_2O$ (30 mM), NaOH (2 M), and 0.2 M Sorbitol at −0.75 V versus HgIHgO followed by annealing in the S vapor at 450–500 °C for 30 min. The XRD confirmed the formation of wittichenite phase of Cu_3BiS_3, and the cathodic photocurrent response showed *p*-type conductivity. Further, Colombara et al. [52] reported a novel low-cost method for formation of Cu_3BiS_3 thin films as an absorber layer in solar cell. Firstly, Cu:Bi 3:1 thin films from an aqueous solution onto Mo-coated glass [53] substrate was prepared. These metal precursor films were converted into Cu_3BiS_3 by adopting sulfurization process. The higher annealing temperature would promote the diffusion of the binary sulfide and enhance the crystallinity of the films.

Recently, the same research group [54] had prepared Cu_3BiS_3 thin films by conversion of stacked and co-electroplated Bi–Cu metal precursors in the presence of elemental sulfur vapor. The precursor solution contained 0.03 M $CuSO_4$, 0.01 M $Bi(NO_3)_3$, 2 M NaOH, and 0.1 M D-sorbitol, and the electrolytic cell used was a three-electrode configuration. Colombara et al. [54] reported the homogeneous and compact Cu_3BiS_3 film formation by sulfurization of the co-deposited (Cu_3Bi) precursors at 500 °C for 0.5 h. The acceptor density and band gap energy of Cu_3BiS_3 was reported 3.10^{17} cm^{-3} and 1.3–1.4 eV, respectively.

Chemical bath deposition technique

A number of research groups reported the successful synthesis of Cu_3BiS_3 thin films for solar cell application by various techniques. However, still there was no single report on the synthesis of Cu_3BiS_3 thin-film-based solar cells using chemical bath deposition technique. Thereby, bearing in mind todays need of low-cost, high-efficiency solar cells, Deshmukh et al. [55] introduced first time

chemical bath deposition technique in the preparation of Cu_3BiS_3 thin films for solar cell applications. The chemical bath deposition technique does not require any sophisticated instrumentation like vacuum systems and other expensive equipment's. The initial chemicals are commonly available and are cheaper materials. With CBD, a large number of substrates can be coated in a single run with a proper jig design. For the synthesis of Cu_3BiS_3 thin films on glass substrate, copper (II) acetate, bismuth (III) nitrate pentahydrate, and thiourea were employed by Deshmukh et al. The as-deposited Cu_3BiS_3 thin films had a direct band gap between 1.56–1.58 eV and absorption coefficient $\sim 10^5$ cm^{-1}. SEM images showed the formation of nanoparticles having diameter 70–80 nm. The atomic ratio of Cu:Bi:S was reported 41:13:45 which is closed to the stoichiometry of Cu_3BiS_3. The optical study directed that the Cu_3BiS_3 films could be applied in thin-film solar cells as an absorber layer.

Spin-coating deposition technique

Spin-coating technique is very simple and low cost for the deposition of various semiconductor thin films. It involves the three steps in the deposition of Cu_3BiS_3 thin films: (1) Preparation of the chemical precursor solution, which contains the ions of interest; (2) spin coating the precursor solution on a substrate to obtain the desired thin film; and (3) annealing the thin film at suitable atmosphere to form Cu_3BiS_3 material. Recently, Zhang et al. [12] in 2016 for the first time reported the synthesis of Cu_3BiS_3 thin films by sulfurizing the mixed metal oxide precursor film deposited by spin-coating technique. The copper nitrate trihydrate, bismuth nitrate pentahydrate, and 2-methoxyethanol were used as precursor to obtain Cu_3BiS_3 thin films. The XRD pattern confirmed the orthorhombic phase of Cu_3BiS_3 above the sulfurization temperature 420 °C. The band gap energy of the Cu_3BiS_3 thin films varied between 1.15 to 1.10 eV due to the larger grain size at higher annealing temperature. The measurement of Hall effect showed that Cu_3BiS_3 had a *p*-type conductivity with carrier concentration of $5.1 \times 10^{16}/cm^3$ and Hall mobility of 3.73 cm^2/VS.

Non-vacuum-based other deposition techniques

Apart from these standard techniques, there are several non-vacuum or innovative techniques employed by a researcher for the deposition of Cu_3BiS_3. Microwaving is a one process used for the preparation of nanostructured materials. It resolves the problems of temperature and concentration gradients and provides uniform development. By concentrating microwave radiation into the solution, the vibrating electric field applies a force on dissolved species to induce vibrations with dissimilar modes. To avoid over-boiling, cyclic microwave radiation (CMR) was used instead of continuous. In 2011, Aup-Ngoen et al. [56] reported CMR synthesis of Cu_3BiS_3 dendrites using L-cysteine as a sulfur source and a complexing agent. For the synthesis of Cu_3BiS_3 dendrites, 3 mM CuCl and 1 mM $BiCl_3$ were dissolved in 30 mL EG with 3 mM L-cystein ($C_3H_7NO_2S$) to form a solution. Then this solution was irradiated using 300–700 W CMR for 40 cycles. The XRD revealed the formation of orthorhombic phase with strongest intensity peak at 31.3° corresponds to (131) plane of Cu_3BiS_3 and photoluminescence (PL) emission of Cu_3BiS_3 dendrites was blue emission at 367 nm.

Zhong et al. [57] reported a facile biomolecule-assisted solvothermal method for the preparation of flower-like Cu_3BiS_3 nanorods using L-cysteine as sulfur source and a complexing agent. Primary, $CuCl_2{\cdot}2H_2O$ (3 mmol), $Bi(NO_3)_3{\cdot}5H_2O$ (1 mmol), and L-cysteine (3 mmol) were dissolved in 40 mL N_1N-dimethylformamide. This mixed solution was filled into auto clave and heated at 200 °C for 16 h. The SEM showed the formation of flower-like Cu_3BiS_3 structure with nanorods having an average diameter of 150 nm. The Cu_3BiS_3 exhibited four Raman vibrational peaks at $\sim$116, 153, 355, 459 cm^{-1}, and a strong band at 356 nm in PL spectra.

Hot injection solution chemical technique is a well-known approach for the preparation of materials with well-defined shape and size. This technique usually used in the synthesis of semiconductor nanocrystals. In 2013, Yan et al. [58] synthesized wittichenite Cu_3BiS_3 nanocrystals by utilizing a hot-injection method for the first time. For this, the recipe was 2.25 mM copper (II) acetylacetonate, 0.75 mM bismuth (III) nitrate pentahydrate (atom ratio Cu:Bi = 3), and 12 ml oleylamine which were added into a three-neck flask and heated at 140 °C for 1 h. When the temperature was raised up to 220 °C, 2.5 ml OLA containing 1.2 $mol{\cdot}l^{-1}$ sulfur was quickly injected into the three-neck flask. The diameter of the obtained Cu_3BiS_3 nanocrystals ranges from 8 to 11 nm with a band gap of 1.56 eV. Raman spectra at 486 and 122 cm^{-1} confirmed the existence of Cu_3BiS_3. Also, Cu_3BiS_3 showed a good photoresponse in I–V experiments.

Hu et al. [59] reported a simple and low-cost screen-printing approach for the preparation of the Cu_3BiS_3 absorber layer. For the formation of the Cu_3BiS_3 composite coating, Bi_2S_3 and CuS powders obtained by CBD were used. The as-deposited CuS and Bi_2S_3 powders were mixed with polyacrylic acid, acting as a binder, and resulting mixture was used as a paste to form Cu_3BiS_3 composite coating. When the annealing temperature was equal or higher than 250 °C, there was an interfacial diffusion of

atoms at the CuS–Bi_2S_3 interface leads to the formation of ternary compound Cu_3BiS_3. The sheet resistance and electrical conductivity of Cu_3BiS_3 annealed in nitrogen was reported 10^3 Ω/□ and 1 S cm^{-1}, respectively. The proposed reaction mechanism for the formation of Cu_3BiS_3 is as follows:

$$6CuS + Bi_2S_3 \rightarrow 2Cu_3BiS_3 + 3S \uparrow \quad (7)$$

Recently, low-temperature solution methods such as solvothermal or hydrothermal have been employed for the synthesis of Cu_3BiS_3 nanocrystallites, but this requires a long reaction time to ensure the well crystallinity of the Cu_3BiS_3. Shen et al. [60] in 2003 described the rapid synthesis of Cu_3BiS_3 at low temperature (195 °C) via a rapid polyol process from single source precursors. For this, a stoichiometric mixture of $Bi(S_2CNEt_2)_3$, $Cu(S_2CNEt_2)_2$, and sodium diethyldithiocarbonate was placed into a three-neck flask which contained 50 ml EG. This system was heated and maintained at 195 °C for 60 min under magnetic stirring. The SEM confirmed the formation of coral shaped nanocrystallites of Cu_3BiS_3 and XRD pattern confirmed the orthorhombic phase.

In 1997, Nair et al. [61] reported the formation of ternary Cu_3BiS_3 during annealing of chemically prepared CuS (0.3 μm) films on Bi_2S_3 (0.1 μm) films. The deposition of Bi_2S_3 was carried out at RT for 2.5 h. containing 10 ml Bi^{3+} (0.5 M), 8 ml TEA (3.7 M), and 8 ml thioacetamide (0.5 M). The CuS was prepared from 10 ml copper (II) chloride (0.5 M), 8 ml TEA (3.7 M), 8 ml 30% aqueous ammonia, 10 ml NaOH (1 M) solution at RT for duration of 3, 5, 8, and 11 h on the coating of Bi_2S_3/glass followed by air annealing in an oven at 100–350 °C for 60 min. The XRD confirmed the formation of wittichenite Cu_3BiS_3 phase. The obtained films were smooth, continuous, and phase-pure. These films were optically absorbing in the visible region (absorption coeff. 4×10^4 cm^{-1} at 2.48 eV) and of the *p*-type with electrical conductivity of 10^2–10^3 Ω^{-1} cm^{-1}.

It is seen that in the above synthesis methods of Cu_3BiS_3, a wide variety of Cu_3BiS_3 crystal morphologies had been described. This included flower-like structure (Fig. 7a, b), nanosheets (Fig. 7c), nanorods (Fig. 7d, e), dendrites (Fig. 7f), flower-like hierarchical structure (Fig. 7g), coral-like nanostructure (Fig. 7h), bent-like nanorods (Fig. 7i), spherical nanoparticles (Fig. 7j), nanoneedle-like (Fig. 7k), and 3D flower-like ball (Fig. 7l), which are presented in Fig. 7. Compared with regular thin films [22], a flower-like, nanosheet, 3D flower-like ball, etc., pattern indicates a high surface area, which has potential applications in the area of energy conversions and sensors [42]. In addition to this, Liang et al. [62] reported the efficiency of solar cells depends on the surface morphology. As per the evidences from SEM micrographs (Fig. 7) of Cu_3BiS_3 thin films, it reveals that such morphologies may be found the potential application as an absorber layer in solar PV cells.

Computational and simulation aspects of Cu_3BiS_3

Till now, it has been reported that Cu_3BiS_3 has a direct band gap in the range of 1.10–1.86 eV [12, 13] and a *p*-type conductivity with a carrier concentration of 2×10^{16} cm^{-3}, which are the appropriate properties for an absorber material in photovoltaics. However, thin-film PVs based on Cu_3BiS_3 are not yet extended to the device level. This is mainly due to the fundamental physical properties of Cu_3BiS_3 are not yet well understood and the quality of the thin film is not optimized. Henceforth, it is necessary to understand the details in the optical and electronic properties for the improvement of PV solar cells based on Cu_3BiS_3.

Yu et al. [63] presented a fundamental analysis of the factors for Cu–V–VI (V=P, As, Bi, Sb; VI–S, Se) system that control absorption strength using the density function theory (DFT) approach. It was reported that the high-valence Cu–V^{5+}–VI compounds have stronger absorption than high-valence $CuIn^{3+}Se_2$. The Cu_3–V–VI semiconductor absorbers contain many members exhibiting spectroscopic limited maximum efficiency (SLME) > 23% at a film thickness of 200 nm. This inherent efficiency, coupled with tunable band gaps, useful electrical properties, makes Cu_3–V–VI family materials attractive as potential candidates for investigation and development of new single-junction solar cell. Later on, Tablero [8] studied the electronic properties of Cu_3BiS_3 by using first-principles density functional method. He had reported maximum efficiency obtained for Cu_3BiS_3:O with the results of generalized gradient approximation (GGA) and local density approximation (LDA) first-principles calculations was 50%. This obtained supreme efficiency is larger than the efficiency of a Cu_3BiS_3 single-junction solar cell with equivalent solar concentration.

Further, Kumar and Persson [64, 65] analyzed the structural, optical, and electronic properties of Cu_3BiS_3 using a first-principles approach within the DFT. It was found that the compound Cu_3BiS_3 has an indirect band gap of Eg = 1.5–1.7 eV. The analysis revealed that Cu_3BiS_3 has a stronger absorption coefficient than other Cu–S based materials like Cu_2ZnSnS_4 and $CuInS_2$. The stronger absorption in Cu_3BiS_3 was explained by the localized Bi 6*p* states in the lowest conduction band, forming a flat energy band that increases the absorption coefficient in the lower energy region. Hence, Cu_3BiS_3 can be regarded as a potential absorber material in thin-film PV technologies.

Recently, Mesa et al. [66] first time used the finite elemental method to simulate the nucleation of dislocations of

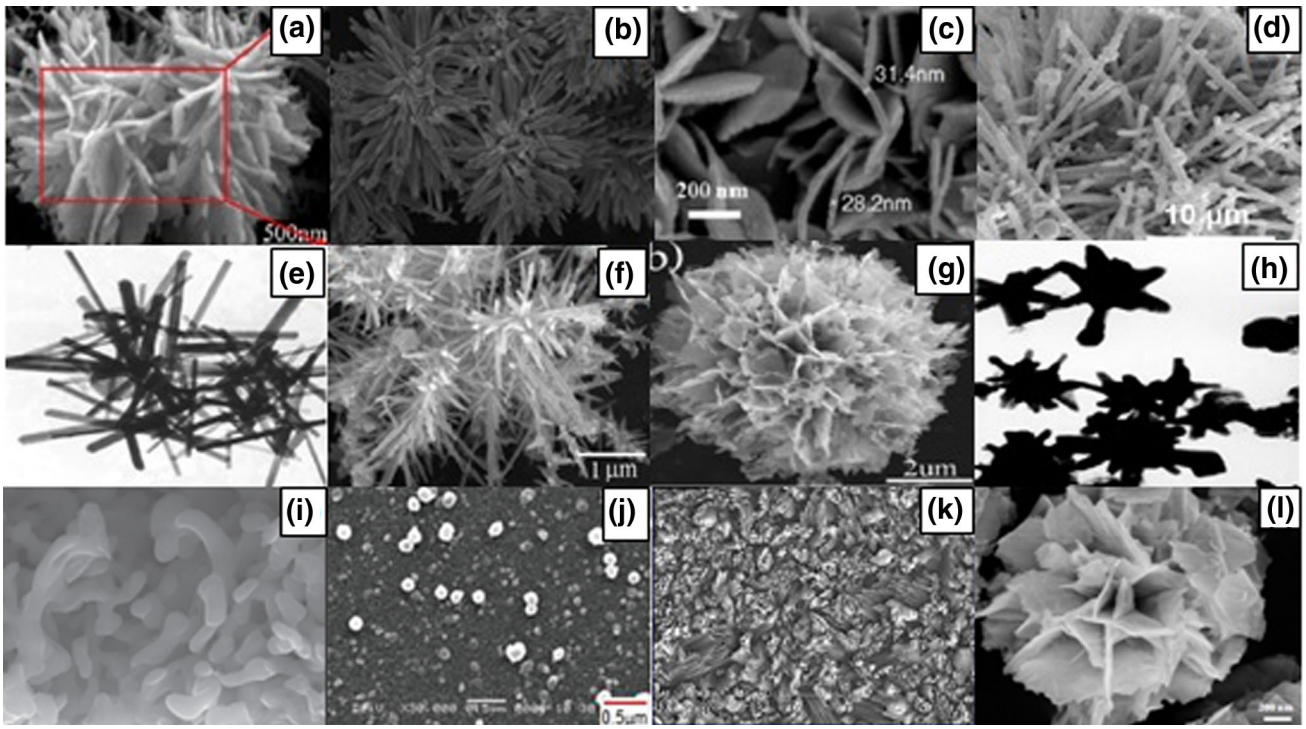

Fig. 7 Flower-like (**a**, **b**) [43, 57]; nanosheets (**c**) [42]; nanorods (**d**, **e**) [37, 47]; dendrites (**f**) [56]; flower-like hierarchical (**g**) [38]; coral-like (**h**) [60]; bent-like nanorods (**i**) [39]; spherical nanoparticles (**j**) [55]; nanoneedle-like (**k**) [29] and 3D flower-like ball (**l**) [45] morphologies of Cu_3BiS_3

Cu_3BiS_3 thin films. They reported the critical thickness of the thin films of Cu_3BiS_3 through the finite element method was 6**b**. Today, the wxAMPS tool is an important application for simulating solar cells with high reliability. In wxAMPS, the obtained values are, $V_{OC} = 0.712$ V, $J_{SC} = 36.25$ mA/cm^2, $FF = 79.54\%$, and an efficiency of 19.86%, which allows Cu_3BiS_3 is an outstanding alternative new material for the designing of photovoltaic devices. This is the first report on the efficiency of Cu_3BiS_3 thin-film-based solar cells using simulation.

Conclusions

A comprehensive review of synthesis, characterizations, processing, and device applications of Cu_3BiS_3 is presented here. The recent significant progress in Cu_3BiS_3 has shown the feasibility of developing photovoltaic solar cells with low-cost, abundant, and/or readily available elements. A broad range of methods, including vacuum as well as non-vacuum-based approaches, have been explored to deposit the Cu_3BiS_3 thin films. This progressive improvement in orthorhombic based pure Cu_3BiS_3 thin film solar cell leads to a highest efficiency of 1.281%. However, this efficiency is very low as compared to its counterpart CIGS, CZTS, CdTe, and CIS thin-film-based solar cells, which are already at the commercialization stage exhibiting the conversion efficiency greater than 14%.

In order to improve the efficiency of Cu_3BiS_3 based thin film solar cells, a more detailed understanding of the fundamental properties of Cu_3BiS_3, particularly the nature of the defects as well as their impact on the properties of Cu_3BiS_3 material is important. It is also essential to detect the secondary phases and their effects in order to optimize the synthesis process to make Cu_3BiS_3 thin films with preferred properties. To develop the successful technology, the detailed understanding of Cu_3BiS_3 material synthesis is necessary. This can be achieved by studying material experimentally as well as theoretically. Also for the long-term durability of wittichenite-based Cu_3BiS_3, thin-film solar cell device under light, moisture, and heat should be studied to form a low-cost, environment-friendly, and high-output approach for the deposition of Cu_3BiS_3 thin films.

This review presents the results on Cu_3BiS_3 thin-film properties as well as its applications in solar cell devices observed at an early stage, which subsequently suggests that it is new and efficient material for low-cost PV solar cells. However, the progress of chemical methods suitable for the synthesis of a ternary Cu_3BiS_3 still remains a major challenge. The wide range of techniques that have been employed to prepare Cu_3BiS_3 semiconductor material had been reviewed with the hope of distinguishing new

paths for productive research based on the present author's work.

Compliance with ethical standards

Conflict of interest The authors declare that they have no conflict of interest.

References

1. Solar Frontier's a conversion efficiency record for CIS thin-film solar cells is 22.3% (2017). http://www.pv-tech.org/news/solar-frontiers-record-efficiency-22.3-cis-cell-faces-global-market-challen. Accessed 17 Feb 2017
2. Yang R, Wang D, Wanb L, Wang D (2014) High-efficiency CdTe thin-film solar cell with a mono-grained CdS window layer. RSC Adv 4:22162–22171
3. First solar sets new world record for CdTe solar cell efficiency (2017). http://investor.firstsolar.com/releasedetail.cfm?Release. Accessed 17 Feb 2017
4. Jackson P, Hariskos D, Lotter E et al (2011) New world record efficiency for Cu(In, Ga)Se_2 thin-film solar cells beyond 20%. Prog Photovolt Res Appl 19:894–897
5. Mitzi DB, Yuan M, Liu W et al (2008) A high-efficiency solution-deposited thin-film photovoltaic device. Adv Mater 20:3657–3662. doi:10.1002/adma.200800555
6. U. S. Geological Survey (2014) Mineral commodity summaries. 30–31 and 74–75
7. Nuffield EW (1947) Studies of mineral sulpho-salts; XI, Wittichenite (klaprothite). Econ Geol 42:147–160
8. Tablero C (2012) Photovoltaic application of O-doped Wittichenite–Cu_3BiS_3: from microscopic properties to maximum efficiencies. Prog Photovolt: Res Appl 21:894–899
9. Kocman V, Nuffield EW (1973) The crystal structure of wittichenite Cu_3BiS_3. Acta Cryst B29:2528–2535
10. Villars P, Prince A, Okamoto H (1994) Handbook of ternary alloy phase diagram, vol 5. ASM International, Materials Park, p 6148
11. Gerein NJ, Haber JA (2006) One-step synthesis, optical and electrical properties of thin film Cu_3BiS_3 for use as a solar absorber in photovoltaic devices. Chem Mater 18:6297–6302
12. Zhang L, Jin X, Yuan C et al (2016) The effect of the sulfur concentration on the phase transformation from the mixed CuO–Bi_2O_3 system to Cu_3BiS_3 during the sulfurization process. Appl Surf Sci 389:858–864
13. Murali B, Krupanidhi SB (2013) Tailoring the band gap and transport properties of Cu_3BiS_3 nanopowders for photodetector applications. J Nanosci Nanotechnol 13:3901–3909
14. Chamorro W, Mesa F, Hurtado M, Gordillo G (2010) Study of structural and morphological properties of ZnS films deposited on Cu_3BiS_3. In: 25th European photovoltaic solar energy conference and exhibition, 6–10 Sept. 2010, Spain, pp 575–579. doi: 10.4229/25thEUPVSEC2010-1DV.3.8
15. Gerein NJ, Haber JA (2006) Synthesis of Cu_3BiS_3 thin films by heating metal and metal sulfide precursor films under hydrogen sulfide. Chem Mater 18:6289–6296
16. Yakushev MV, Maiello P, Raadik T et al (2014) Electronic and structural characterization of Cu_3BiS_3 thin films for the absorber layer of sustainable photovoltaics. Thin Solid Films 562:195–199
17. Yakushev MV, Maiello P, Raadik T et al (2014) Investigation of the structural, optical and electrical properties of Cu_3BiS_3 semiconducting thin films. Energy Proced 60:166–172
18. Hussain KMA, Mahmood ZH, Syed IM et al (2014) Thermal vacuum deposition of cadmium telluride thin films solar cell material. Am J Mater Sci Appl 2:91–95
19. Ko BS, Sung SJ, Kim DH et al (2013) Effects of annealing on structural and electrical properties of sub-micron thick CIGS films. Curr Appl Phys 13:S135–S139
20. Li Y, Chen J, Ma J (2015) Properties of Cu_2ZnSnS_4 (CZTS) thin films prepared by plasma assisted co-evaporation. J Mater Sci: Mater Electron 26:6546–6551
21. Mesa F, Gordillo G (2009) Effect of preparation condition on the properties of Cu_3BiS_3 thin films grown by a two-step process. J Physics Conf Ser 167:012019-5
22. Mesa F, Dussan A, Gordillo G (2009) Evidence of trapping and photoelectric properties of Cu_3BiS_3 thin films. Phys B 404:5227–5230
23. Mesa F, Dussan A, Gordillo G (2010) Study of the growth process and opto-electrical properties of nanocrystalline Cu_3BiS_3 thin films. Phys Status Solidi C 7:917–920
24. Mesa F, Gordillo G, Dittrich T et al (2010) Transient surface photovoltage of p-type Cu_3BiS_3. Appl Phys Lett 96:082113
25. Mesa F, Chamorro W, Vallejo W et al (2012) Junction formation of Cu_3BiS_3 investigated by Kelvin probe Force microscopy and surface photovoltage measurements. Beilstein J Nanotechnol 3:277–284
26. Romero E, Vallejo W, Gordillo G (2008) Comparative study of ZnS thin films deposited by CBD and co-evaporation. In: Proceeding of 33rd IEEE photovoltaic specialist conference, San Diego, USA, IEEE: Piscataway, NJ
27. Mesa F, Dussan A, Sandino J, Lichte H (2012) Characterization of Al/Cu_3BiS_3/buffer/ZnO solar cells structure by TEM. J Nanoparts Res 14:1054
28. Dussan A, Murillo JM, Mesa F (2012) Thermally stimulated conductivity of Cu_3BiS_3 thin films deposited by co-evaporation: determination of trap parameters related to defects in the gap. J Mater Sci 47:6688–6692
29. Murali B, Madhuri M, Krupanidhi SB (2014) Near-infrared photoactive Cu_3BiS_3 thin films by co-evaporation. J Appl Phys 115:173109
30. Mesa F, Dussan A, Paez-Sierra BA, Rodriguez-Hernandez H (2014) Hall effect and transient surface photovoltage (SPV) study of Cu_3BiS_3 thin films. Univ Sci 19:99–105
31. Mesa F, Chamorro W, Hurtado M (2015) Optical and structural study of In_2S_3 thin films grown by co-evaporation and chemical bath deposition (CBD) on Cu_3BiS_3. Appl Surf Sci 350:38–42
32. Estrella V, Nair MTS, Nair PK (2003) Semiconducting Cu_3BiS_3 thin films formed by the solid state reaction of CuS and bismuth thin films. Semicond Sci Technol 18:190–194
33. Nikale VM, Shinde SS, Bhosale CH et al (2011) Physical properties of spray deposited CdTe thin films: PEC performance. J Semicond 32:033001
34. Gu S, Shin HS, Yeo DH et al (2011) Synthesis of the single phase CIGS particle by solvothermal method for solar cell application. Curr Appl Phys 11:S99–S102
35. Patel K, Shah DV, Kheraj V (2015) Influence of deposition parameters and annealing on Cu_2ZnSnS_4 thin films grown by SILAR. J Alloys Compd 622:942–947
36. Liu S, Wang X, Nie L, Chen L, Yuan R (2015) Spray pyrolysis deposition of Cu_3BiS_3 thin films. Thin Solid Films 585:72–75
37. Yan J, Yu J, Zhang W et al (2012) Synthesis of Cu_3BiS_3 and $AgBiS_2$ crystallites with controlled morphology using hypocerllin template and their catalytic role in the polymerization of alkylsilane. J Mater Sci 47:4159–4166
38. Zeng Y, Li H, Qu B et al (2012) Facile synthesis of flower-like Cu_3BiS_3 hierarchical nanostructure and their electrochemical properties for lithium-ion batteries. Cryst Eng Comm 14:550–554

39. Murali B, Venugopal R, Chandan KG, Krupanidhi SB (2012) Solvothermal synthesis, structural and optical properties of phase-pure Cu_3BiS_3 nano-powders exhibiting near-IR photodetection. Adv Sci Eng Med 4:89–95
40. Viezbicke BD, Birnie DP (2013) Solvothermal synthesis of Cu_3BiS_3 enabled by precursor complexing. ACS Sustain Chem Eng 1:306–308
41. Murali B, Krupanidhi SB (2015) Nanocomposite based organic-inorganic Cu_3BiS_3 high sensitive hybrid photonic devices. J Nanosci Nanotechnol 15:2742–2752
42. Yin J, Jia J (2014) Synthesis of Cu_3BiS_3 nanosheet films on TiO_2 nanorod arrays by solvothermal route and their photoelectrochemical characteristics. Cryst Eng Comm 16:2795–2801
43. Zhong JS, Wang QY, Zhu X et al (2015) Solvothermal synthesis of flower-like Cu_3BiS_3 sensitized TiO_2 nanotube arrays for enhancing photo electrochemical performance. J Alloys Compd 641:144–147
44. Santhanapriya R, Muthukannan A, Sivakumar G, Mohanraj K (2016) Solvothermal-assisted synthesis of Cu_3XS_3 (X = Bi and Sb) chalcogenide nanoparticles. Synth React Inorg Met-Org Nano-Met Chem 46:1388–1394
45. Gao X, Wang Y, Ma Z et al (2016) A ternary sulphonium composite Cu_3BiS_3/S as cathode materials for lithium–sulfur batteries. J Mater Sci 51:5139–5145
46. Hu J, Deng B, Wang C et al (2003) Convenient hydrothermal decomposition process for preparation of nanocrystalline mineral Cu_3BiS_3 and $Pb_{1-x}Bi_{2x/3}S$. Mater Chem Phys 78:650–654
47. Chen D, Shen G, Tang K et al (2003) The synthesis of Cu_3BiS_3 nanorods via a simple ethanol-thermal route. J Cryst Growth 253:512–516
48. Malaquias JC, Berg DM et al (2015) Controlled bandgap $CuIn_{1-x}Ga_x$ $(S_{0.1}Se_{0.9})_2$ $(0.10 \leq x \leq 0.72)$ solar cells from electrodeposited precursor. Thin Solid Films 582:2–6
49. Shin S, Park C, Kim C et al (2016) Cyclic voltammetry studies of copper, tin and zinc electrodeposition in a citrate complex system for CZTS solar cell application. Curr Appl Phys 16:207–210
50. Echendu OK, Fauzi F, Weerasinghe AR, Dharmadasa IM (2014) High short-circuit current density CdTe solar cells using all-electrodeposited semiconductors. Thin Solid Films 556:529–534
51. Peter LM, Scragg JJ, Loken A, Dale PJ (2009) Towards sustainable photovoltaic solar energy conversion: studies of new absorber materials. ECS Trans 19:179
52. Colombara D, Peter LM, Rogers KD, Hutchings K (2012) Thermochemical and kinetic aspects of the sulfurization of Cu–Sb and Cu–Bi thin films. J Solid State Chem 186:36–46
53. Colombara D, Peter LM, Rogers KD et al (2011) Formation of $CuSbS_2$ and $CuSbSe_2$ thin films via chalcogenisation of Sb–Cu metal precursors. Thin Solid Films 519:7438–7443
54. Colombara D, Peter LM, Hutchings K et al (2012) Formation of Cu_3BiS_3 thin films via sulfurization of Bi–Cu metal precursors. Thin Solid Films 520:5165–5171
55. Deshmukh SG, Panchal AK, Kheraj V (2016) Chemical bath deposition of Cu_3BiS_3 thin films. In: AIP conference proceedings 1728:020023-1- 020033-5. doi: 10.1063/1.4946073
56. Aup-Ngoen K, Thongtem S, Thongtem T (2011) Cyclic microwave-assisted synthesis of Cu_3BiS_3 dendrites using L-cysteine as a sulfur source and complexing agent. Mater Lett 65:442–445
57. Zhong J, Xiang W, Cai Q et al (2012) Synthesis, characterization and optical properties of flower-like Cu_3BiS_3 nanorods. Mater Lett 70:63–66
58. Yan C, Gu E, Liu F et al (2013) Colloidal synthesis and characterizations of wittichenite copper bismuth sulphide nanocrystals. Nanoscale 5:1789–1792
59. Hu H, Gomez-Daza O, Nair PK (1998) Screen-printed Cu_3BiS_3-polyacrylic acid composite coating. J Mater Res 13:2453–2456
60. Shen G, Chen D, Tang K, Qian Y (2003) Synthesis of ternary sulfides Cu(Ag)–Bi–S coral-shaped crystals from single-source precursors. J Cryst Growth 257:293–296
61. Nair PK, Huang L, Nair MTS et al (1997) Formation of P-type Cu_3BiS_3 absorber thin films by annealing chemically deposited Bi_2S_3–CuS thin films. J Mater Res 12:651–656
62. Liang Z, Zhang Q, Wiranwetchayan O et al (2012) Effects of the morphology of a ZnO buffer layer on the photovoltaic performance of inverted polymer solar cells. Adv Funct Mater 22:2194–2201
63. Liping Y, Kokenyesi RS, Keszler DA et al (2012) Inverse design of high absorption thin-film photovoltaic materials. Adv Energy Mater 3:43–48
64. Kumar M, Persson C (2013) Cu_3BiS_3 as a potential photovoltaic absorber with high optical efficiency. Appl Phys Lett 102:062109
65. Kumar M, Persson C (2013) Ternary Cu_3BiY_3 (Y=S, Se and Te) for thin-film solar cells. Mater Res Soc 1538:235–240
66. Mesa F, Ballesteros V, Dussan A (2014) Growth analysis and numerical simulation of Cu_3BiS_3 absorbing layer solar cell through the wxAMPS and finite element method. Acta Phys Polon A 125:385–387